



CHORUS

This is the accepted manuscript made available via CHORUS. The article has been published as:

Prediction of a $\text{Ca}(\text{BH}_{4})(\text{NH}_{2})$ quaternary hydrogen storage compound from first-principles calculations

Dilpuneet S. Aidhy, Yongsheng Zhang, and C. Wolverton

Phys. Rev. B **84**, 134103 — Published 14 October 2011

DOI: [10.1103/PhysRevB.84.134103](https://doi.org/10.1103/PhysRevB.84.134103)

Prediction of a $\text{Ca}(\text{BH}_4)(\text{NH}_2)$ quaternary hydrogen storage compound from
first-principles calculations

Dilpuneet S. Aidhy*, Yongsheng Zhang and C. Wolverton[#]
Department of Materials Science and Engineering, Northwestern University, IL 60208.

*Current address:
IBM India,
Manyata Technological Park,
Bangalore, 560045.
India.
Email: dilaidhy@in.ibm.com.

[#]Corresponding author
Email: c-wolverton@northwestern.edu

Abstract

We use a combination of density functional theory (DFT) calculations, and a Monte Carlo based crystal structure prediction tool, the Prototype Electrostatic Ground State (PEGS) method, to search for new hydrogen storage compounds in the Ca based mixed amide-borohydride quaternary system. We predict the existence of a new ordered quaternary compound, CaBNH_6 , whose stoichiometry comes from a 1:1 mixture of $\text{Ca}(\text{BH}_4)_2$ and $\text{Ca}(\text{NH}_2)_2$. Our DFT calculations show that CaBNH_6 is ~ 12.5 kJ/mol Ca (at $T = 0$ K) lower in energy than the mixture of $1/2[\text{Ca}(\text{BH}_4)_2 + \text{Ca}(\text{NH}_2)_2]$. DFT phonon calculations of vibrational thermodynamics show that this stability of CaBNH_6 [with respect to $\text{Ca}(\text{BH}_4)_2$ and $\text{Ca}(\text{NH}_2)_2$] persists to finite temperatures. The predicted crystal structure contains two formula units of CaBNH_6 . We have also performed a thermodynamic analysis of hydrogen decomposition of our predicted compound using the Grand Canonical Linear Programming (GCLP) method combined with a large database of DFT energies and vibrational thermodynamics. We find that the thermodynamically preferred decomposition reaction for CaBNH_6 involves formation of BN with a low decomposition enthalpy. Though the decomposition enthalpy is low, the kinetic behavior of CaBNH_6 decomposition is not yet known. We assert that further experimental investigation of this system is warranted to verify the existence of predicted quaternary compounds in this Ca-B-N-H system, as well as to elucidate their hydrogen release reaction pathways.

1. Introduction

A practical hydrogen storage material for fuel cell applications would have high hydrogen storage capacity, both gravimetrically and volumetrically, fast kinetics for hydrogen release, and reversibility. In search of this material, various material classes have been proposed as candidates such as conventional metal hydrides, complex hydrides, sorbents and chemical hydrides.^{1,2,3,4,5,6,7,8,9,10} Although materials in these classes often possess some of the desired properties, a single material that encompasses all of them has remained undiscovered.

Complex hydrides have received significant attention due to their high hydrogen storage capacities. One particular compound, $\text{Li}_4\text{BN}_3\text{H}_{10}$, a 1:3 mixture of LiBH_4 and LiNH_2 , has stimulated interest due to its measured $\sim 11.9\text{wt}\%$ hydrogen release.^{11,12,13,14,15,16,17,18,19} $\text{Li}_4\text{BN}_3\text{H}_{10}$ releases hydrogen via a weak endothermic reaction by forming Li_3BN_2 .^{11,14} However, while the decomposition reaction is weakly endothermic, high temperatures ($\sim 520\text{ K}$) are required to decompose $\text{Li}_4\text{BN}_3\text{H}_{10}$, illustrating the fact that hydrogen storage in this compound is hampered by kinetic limitations.¹¹ Efforts are ongoing to elucidate hydrogen release rate-limiting steps¹⁸ as well as further enhance the hydrogen-release kinetics in $\text{Li}_4\text{BN}_3\text{H}_{10}$.²⁰

Exploring new materials in the family of mixed amide-borohydrides may not only provide new promising hydrogen-storage reactions but could also provide further understanding of this class of systems in general. To our knowledge, we note that apart from two Li-based compounds, i.e., Li_2BNH_6 and $\text{Li}_4\text{BN}_3\text{H}_{10}$, no other mixed amide-borohydride compound has been reported. In this paper, we use density functional theory

(DFT) to investigate Ca-based mixed amide borohydride compounds. In particular, we consider mixtures of $\text{Ca}(\text{BH}_4)_2$ and $\text{Ca}(\text{NH}_2)_2$ in different compositions and predict the existence of $\text{Ca}(\text{BH}_4)(\text{NH}_2)$, or CaBNH_6 , a new, as-yet-unobserved compound. We predict a low-energy crystal structure for this compound using the prototype electrostatic ground state (PEGS) approach,²¹ a DFT-based approach for crystal structure prediction. Our DFT calculations demonstrate that this compound is stable with respect to decomposition into $\text{Ca}(\text{BH}_4)_2$ and $\text{Ca}(\text{NH}_2)_2$. By combining DFT with the grand-canonical linear programming (GCLP) tool,²² we are able to predict the low-energy **thermodynamic** decomposition pathway of this compound. We find that the thermodynamically preferred decomposition reaction for CaBNH_6 involves formation of BN with a low decomposition enthalpy. We also compare the stability and decomposition of the predicted CaBNH_6 phase with the observed properties of the $\text{Li}_4\text{BN}_3\text{H}_{10}$ compound. Further experimental investigation of this system is called for to verify the existence of predicted quaternary compounds in this Ca-B-N-H system, as well as to elucidate their hydrogen release reaction pathways.

2. Methodology

DFT calculations have been used to calculate a wide range of properties for many hydrogen-storage materials.^{14,18,23,24,25,26,27,28,29,30,31,32,33,34,35,36,37,38,39,40,41,42,43,44,45,46,47,48,49,50,51,52,53} In these calculations, the *a priori* knowledge of a compound's crystal structure is typically obtained from experiments where the system has already been structurally well characterized. By contrast, for the DFT calculations in this work, the crystal structure information is currently not available. To solve this problem, we have used a recently

developed crystal structure prediction method, known as the prototype electrostatic ground state (PEGS) approach, which has been successfully shown to predict low energy crystal structure for ionically-bonded systems such as alanates,²² borohydrides⁵⁴ and imides.⁵⁵ In addition, this approach has also been used to predict crystal structures for double cation borohydrides, i.e., $M_1M_2(BH_4)_x$ (where M_1 and M_2 represent different metal cations)^{56,57,58} In the present work, for the first time, we use this approach to predict crystal structure of a double anion system, i.e., containing $(BH_4)^-$ and $(NH_2)^-$ units.

In the PEGS approach, energy of a stoichiometric random arrangement of ions enclosed in a box (of arbitrary shape) is minimized using a Monte Carlo (MC) method. The MC method is driven by a combination of pair-wise potentials: ionic point-charge interactions and a soft-sphere repulsion potential

$$E = \sum_{i>j} \frac{q_i q_j}{r_{ij}} + \sum_{i>j} \frac{1}{r_{ij}^{12}} \quad (1)$$

where, q and r is the charge and distance between the two ionic species. In Eq. 1, the first term represents point-charge electrostatic interactions between the ions, and the second term is the soft-sphere repulsion that prevents ionic overlapping. The MC based energy minimization is performed via simulated annealing using four distinct types of Monte Carlo moves: change in lattice vectors (magnitude or direction), cation/anion translations, rotation of the anionic units, e.g., $(BH_4)^-$, and swapping of cation and anion locations. Since PEGS is a stochastic method with the possibility of getting trapped in local minima of the configurational energy space, it requires multiple simulations to adequately sample phase-space configurations. The number of simulations depends on the complexity of the problem and the number of atoms included in the PEGS unit cells.

For each stoichiometry considered, we use ~25 PEGS simulations to search for low-energy structures. Each of these simulations is initialized with a different set of random initial atomic positions.

The input parameters for the PEGS calculations are ionic charge and radii of each species. The ionic charge can be obtained from separate DFT calculations, e.g., Bader charge,⁵⁹ and the ionic radii can be obtained from standard literature sources, e.g., Pauling radii⁶⁰. The structures found from the PEGS calculations can also depend upon the input parameters. We therefore perform PEGS calculations over a range of input parameters - here, we only report the input parameters used for the structure found to ultimately possess the lowest DFT energy. The ionic charges used for Ca, B and N are +2.0 e, +1.54 e, and -1.60 e respectively. The ionic charges used for H are -0.64 e and +0.30e pertaining to the H in (BH₄)⁻ and (NH₂)⁻ units respectively. The ionic radii used are 1.0 Å, 1.83 Å, 1.40 Å for Ca, B and N respectively, and 1.23 Å and 1.43 Å for H in (BH₄)⁻ and (NH₂)⁻ units respectively. The structures obtained from the PEGS simulation are then further relaxed using a more accurate DFT method. The structure with the lowest DFT energy is then used as the “PEGs-predicted” structure, and the stability is tested with respect to decomposition into Ca(BH₄)₂ and Ca(NH₂)₂.

The first-principles DFT calculations are performed using the Vienna *Ab Initio* Simulation Package (VASP).^{61,62} We use generalized gradient approximation (GGA) in PW91 form⁶³ for the exchange and correlation. Total energies are calculated using projector-augmented wave (PAW) potentials⁶⁴ to treat interactions between ions and valence electrons. For high-precision calculations, we use the so-called hard potentials provided in the VASP code. A plane wave energy cut-off of 850 eV is used for the

electronic wave functions, and a 6x6x6 Monkhorst-Pack⁶⁵ k -points mesh is used to sample the Brillouin zone. Atomic positions are relaxed until all forces are less than 0.01 eV/Å. The energies of H₂, N₂ and NH₃ are calculated by placing the molecules in a 10 Å cubic sized box. Finite-temperature vibrational effects are included by evaluating the normal-mode frequencies of ionic vibrations within the harmonic approximation.^{66,67} We use the frozen phonon force constant approach and diagonalize the dynamical matrix extracted from the force constants generated by displacing symmetrically inequivalent atoms about their equilibrium positions by ± 0.03 Å and ± 0.06 Å fitted to cubic splines. The finite-temperature energetics, i.e., H_{vib} and S_{vib} are then calculated from the obtained normal-mode frequencies (ω) by using the following relationships:

$$H_{vib}(T) = \sum_i \frac{1}{2} \hbar \omega_i + \hbar \omega_i \left[\exp\left(\frac{\hbar \omega_i}{k_B T}\right) - 1 \right]^{-1} \quad (2)$$

$$S_{vib}(T) = k_B \sum_i \frac{\hbar \omega_i / k_B T}{\exp(\hbar \omega_i / k_B T) - 1} - \ln \left[1 - \exp\left(\frac{-\hbar \omega_i}{k_B T}\right) \right] \quad (3)$$

where, k_B is the Boltzmann constant and T is the absolute temperature. The zero-point energy ($H_{vib}^{T=0}$) can be obtained by substituting $T = 0$ in Eq. 2.

To determine the lowest energy decomposition reactions, we use the recently developed grand canonical linear programming (GCLP) method. In this method, we start with a collection of solid state phases with phase fractions x_i , assumed to be in contact with hydrogen gas reservoir at chemical potential, $\mu_{H_2}(p, T)$. For a given value of $\mu_{H_2}(p, T)$, we minimize the grand potential, $\Omega(p, T)$, of our collection of phases with respect to the phase fractions x_i , subject to mass-conservation constraints for the non-hydrogen species. The grand potential and mass conservation constraints are given by

$$\Omega(p,T) = \sum_i x_i F_i(T) - \frac{\mu_{H_2}(p,T)}{2} \sum_i x_i n_i^H \quad (4)$$

$$f_s = \sum_i x_i n_i^s = \text{const. for } \forall s \neq H \quad (5)$$

where, $F_i(T)$ is the free energy of phase i , n_i^H is the number of hydrogen atoms in one formula unit of phase i , n_i^s is the number of ions of type s in one formula unit, x_i are the molar fractions of phases coexisting at a given temperature, composition and pressure, and f_s is the molar ratio of non-hydrogen species (eg., Ca, B, N). The free energies, $F_i(T)$, for all phases are obtained from static DFT total energy. Because both the function to be minimized (Eq. 4) and the constraints (Eq. 5) are linear in the variables we seek, the minimization problem can be solved using linear programming. For further details on GCLP, we refer the reader to Ref.[²²]. The following phases are included in this study: Ca, B, H₂, N₂, Ca(NH₂BH₃)₂, Ca₂(BN₂)H, Ca₃BN₃, **Ca₃(BN₂)₂**, Ca₂N, CaB₆ CaB₄, BN, CaH₂, NH₃, CaB₁₂H₁₂, CaB₂H₄, CaB₂H₆, Ca(BH₄)₂, Ca(NH₂)₂, CaN₆, Ca₃N₂, Ca₂NH, CaNH, BH₃NH₃, B₃N₃H₆, (BH₂NH₂)₃, BH₃N₂H₄, (NH₄)₂B₁₂H₁₂, B₂H₆, N₄H₄, B₁₆H₂₀, B₁₈H₂₂, B₂₀H₁₆, B₄H₁₀, B₅H₁₁, B₅H₈, B₆H₁₀, B₈H₁₂, and B₉H₁₅. In addition, we include the new Ca-based mixed amide-borohydride phases predicted in this work.

3. Results

A. Thermodynamics of mixed $x\text{Ca}(\text{BH}_4)_2 + (1-x)\text{Ca}(\text{NH}_2)_2$ compounds

We search for new, potentially stable compounds in the $x\text{Ca}(\text{BH}_4)_2 + (1-x)\text{Ca}(\text{NH}_2)_2$ system. Because no compounds have been reported in this system, not only are the crystal structures unknown, but even the stoichiometries must be predicted. To that end, we search for compounds of three different stoichiometries, corresponding to $x = 0.25, 0.50,$ and 0.75 . In each case, we first assess the stability of the mixed compound

with respect to the individual hydrides, $\text{Ca}(\text{BH}_4)_2$ and $\text{Ca}(\text{NH}_2)_2$. We begin with a discussion of the $x = 0.50$ stoichiometry, CaBNH_6 . For this stoichiometry, we ran ~ 25 PEGS simulations for unit cells comprised of one and two formula units, and found several low energy candidate structures. For our lowest energy CaBNH_6 compound, the formation from $\text{Ca}(\text{BH}_4)_2$ and $\text{Ca}(\text{NH}_2)_2$ is found to be energetically favorable as shown in the “convex-hull” plot in Fig. 1. When plotted in this way, the stability of a compound requires its energy to be on a convex hull, i.e., the compound should be lower in energy than the linear combination of any other phases in the system. The formation energy at $T = 0\text{K}$ is calculated to be, $\Delta E \approx -12.5$ kJ/mol Ca. Our predicted compound has a space group $P\bar{1}$ (# 2). We further find that the PEGS calculations predict two more crystal structures with SG Cc (#9) and Cm (#8) that have negative formation energies of approximately -9 kJ/mol Ca. These relatively large, negative formation energies strongly support our assertion that amide-borohydride mixing is preferred in Ca-based systems.

We have also explored compounds with $x = 0.25$ and $x = 0.75$ compositions between $\text{Ca}(\text{BH}_4)_2$ and $\text{Ca}(\text{NH}_2)_2$, i.e., $\text{Ca}_2\text{B}_3\text{NH}_{14}$ and $\text{Ca}_2\text{BN}_3\text{H}_{10}$ respectively. Having established the existence of the compound with $x = 0.50$ composition, which has similar composition (B:N ratio of 1:1) to that of the observed Li_2BNH_6 phase, we are particularly interested in $\text{Ca}_2\text{BN}_3\text{H}_{10}$ because it has a similar composition (B:N ratio of 1:3) to the observed $\text{Li}_4\text{BN}_3\text{H}_{10}$ phase [containing one $(\text{BH}_4)^-$ and three $(\text{NH}_2)^-$ units]. We carry out ~ 25 different PEGS + DFT calculations containing 1 formula unit for each of the two stoichiometries separately. In contrast to CaBNH_6 , we do not find any structures with negative formation energies for either $\text{Ca}_2\text{B}_3\text{NH}_{14}$ or $\text{Ca}_2\text{BN}_3\text{H}_{10}$. The lowest formation-energy structure for both compounds is nearly zero (slightly positive) for both $\text{Ca}_2\text{B}_3\text{NH}_{14}$

and $\text{Ca}_2\text{BN}_3\text{H}_{10}$ as shown in Fig. 1. We acknowledge that crystal structure prediction tools, such as PEGS, often become more limited for systems with larger numbers of atoms. $\text{Ca}_2\text{B}_3\text{NH}_{14}$ and $\text{Ca}_2\text{BN}_3\text{H}_{10}$ have 20 and 16 atoms in the formula units, respectively compared to 9 in CaBNH_6 . Not only is the calculation for large-sized systems more computationally expensive but the number of possible structural degrees of freedom also increases very rapidly with the number of atoms in the cell. As a result, predicting a true ground state crystal structure becomes a difficult task. To adequately sample the phase space of these large unit cells would thus require a prohibitively large number of PEGS+DFT simulations.

We should note that due to the stochastic nature of the PEGS approach, the predictions we obtain from this method are strictly speaking, only upper bounds to the true ground state energy. In other words, there is always the possibility that even lower energy structures have been missed in our calculations. The fact that we have found compounds with negative formation energies (as an upper bound to the true ground state energies) allows us to confidently predict the existence of as-yet-unobserved compounds in this system. We do acknowledge the possibility that lower energy structures of these compounds (or those of other stoichiometries in this system) may exist in this system.

We next compare the energetics of our predicted CaBNH_6 with the analogous ordering in Li_2BNH_6 and $\text{Li}_4\text{BN}_3\text{H}_{10}$. The former is a 1:1 mixture between LiBH_4 and LiNH_2 , whereas the latter is a 1:3 mixture. For DFT calculations of Li_2BNH_6 and $\text{Li}_4\text{BN}_3\text{H}_{10}$, we use the $R\bar{3}$ ⁶⁸ and $I2_13$ ^{69,70} crystal structures respectively. The formation energies (the energies with respect to the composition-weighted average of LiBH_4 and LiNH_2) are found to be -4.5 kJ/mol Li and -2.8 kJ/mol Li for Li_2BNH_6 and $\text{Li}_4\text{BN}_3\text{H}_{10}$

respectively. Both formation energies lie on a convex hull in the $\text{LiBH}_4/\text{LiNH}_2$ system, which is consistent with the experimental reports of their stability. In comparison of CaBNH_6 with Li_2BNH_6 , we find that CaBNH_6 is even more stable, having a formation energy of -12.5 kJ/mol Ca compared to -4.5 kJ/mol Li. This comparison again underscores the validity of our prediction of ordering in this Ca amide/borohydride system, and we suggest that future experiments are warranted to search for stable new phases in this system.

To further elucidate the stability of CaBNH_6 , we calculate the contribution of vibrational thermodynamics to the formation enthalpy. The enthalpy of formation $\Delta H_f(T)$ entropy of formation, $\Delta S_f(T)$, and the free energy of formation, $\Delta G_f(T)$, are obtained using the following relationships:

$$\Delta H_f(T) = H(T)_{\text{CaBNH}_6} - [H(T)_{\text{Ca}(\text{BH}_4)_2} + H(T)_{\text{Ca}(\text{NH}_2)_2}] \quad (4)$$

$$\Delta S_f(T) = S(T)_{\text{CaBNH}_6} - [S(T)_{\text{Ca}(\text{BH}_4)_2} + S(T)_{\text{Ca}(\text{NH}_2)_2}] \quad (5)$$

$$\Delta G_f(T) = \Delta H_f(T) - T\Delta S_f(T) \quad (6)$$

The calculated value of $\Delta G_f(T)$ is shown in Fig. 2. The effect of zero-point vibrations increases the value of the formation energy from -12.5 kJ/mol Ca to approximately -7.5 kJ/mol Ca. The thermal contributions of vibrations also serve to slightly destabilize the compound, so that by 400K, the free energy of formation is about -6 kJ/mol Ca. However, through the entire temperature range, the predicted crystal structure is stable with respect to decomposition into $\text{Ca}(\text{BH}_4)_2 + \text{Ca}(\text{NH}_2)_2$. (We will examine below the stability with respect to H_2 release.)

B. Crystal structure of the predicted CaBNH₆ compound

We now turn our attention to the crystal structure of CaBNH₆. The predicted lowest energy crystal structure is $P\bar{1}$ (#2). It contains two formula units of CaBNH₆. The lattice parameters are $a = 5.038 \text{ \AA}$, $b = 5.652 \text{ \AA}$, and $c = 6.956 \text{ \AA}$, and the cell angles are $\alpha = 69.56^\circ$, $\beta = 71.12^\circ$ and $\gamma = 88.93^\circ$. The Wyckoff parameters and the internal atomic coordinates of the crystal structure are given in Table 1, and the schematic illustration of the crystal structure is given in Fig. 3. The predicted interatomic bond lengths of CaBNH₆ and their comparison to the DFT calculated bond lengths in Li₂BNH₆ and Li₄BN₃H₁₀¹⁴ are given in Table 2. We note that both the B-H and N-H bond lengths are very similar to the DFT calculated bond lengths in Li₂BNH₆ and Li₄BN₃H₁₀¹⁴. In contrast, we find that the B-cation and N-cation distances are larger in Ca-based system compared to Li-based systems. These cation-anion distances vary significantly between the Li and Ca systems due to the difference in the ionic radii of the cations (0.68 Å for Li to 0.99 Å for Ca). As expected, due to larger-sized Ca, the Ca-B and Ca-N distances are larger.

C. Decomposition reaction pathways and energies of CaBNH₆

In this section, we calculate the hydrogen release **thermodynamic** pathways using a combination of DFT thermodynamics and the GCLP methodology.²² Before discussing CaBNH₆, we revisit the thermodynamic properties of Li₄BN₃H₁₀, particularly highlighting the comparison between DFT calculations and experimental observation for the decomposition reactions of this compound. In the original work reporting the existence of Li₄BN₃H₁₀, Pinkerton *et al.* found that the quaternary compound decomposes via forming Li₃BN₂ + H₂ releasing 11.9 wt.% H₂.¹¹ Subsequent DFT results¹⁴ were consistent with experiments in demonstrating that Li₃BN₂ is a stable reaction product at

elevated temperatures. However, in addition to Li_3BN_2 , the DFT calculations also predicted LiNH_2 as a decomposition product.¹⁴ This difference was due to the fact that in the experiments of Ref. 11, an off-stoichiometric version of $\text{Li}_4\text{BN}_3\text{H}_{10}$ was synthesized, formed from a 1:2 ratio of LiBH_4 and LiNH_2 rather than 1:3. The DFT calculations, in general, agreed very well with the experimental results for both decomposition pathway and decomposition thermodynamics.

In the previous DFT study¹⁴ of the decomposition of $\text{Li}_4\text{BN}_3\text{H}_{10}$ Siegel et al. performed a computational search over 17 candidate dehydrogenation reactions, and identified three reactions having favorable thermodynamics spanning the temperature range $T = 0\text{--}1000$ K. Specifically, the two reactions that were found at ambient pressure and low temperature conditions are:



Reaction (2) is consistent with the decomposition experiments, which find a Li_3BN_2 product at temperatures above 500 K.¹¹ The predicted lower temperature reaction (1) with a BN product is not observed experimentally, presumably due to kinetic limitations.

Since CaBNH_6 belongs to a similar material system as $\text{Li}_4\text{BN}_3\text{H}_{10}$, one might expect similar decomposition pathways. From our GCLP calculations, we find that the preferred low-temperature hydrogen release reaction for CaBNH_6 is indeed similar to reaction (1), i.e.,



with a volumetric density of 76.68 g H_2/L .

In both reactions (1) and (3), the decomposition products involve a hydride, BN, and H₂. The formation of LiNH₂ as a decomposition product in Reaction (1) is due to the fact that the B:N ratio is not 1 in the Li₄BN₃H₁₀ compound. However, the ratio B:N=1 in CaBNH₆, hence the decomposition reaction (3) involves only a stoichiometric BN product, but no residual amide or borohydride.

We compare the thermodynamics of reactions (1) and (3) in Table 3. We find that the values of the thermodynamic quantities for the CaBNH₆ decomposition are very similar to those of Li₄BN₃H₁₀ (taken from Ref. 14) At T = 0 K, the DFT calculated change in static enthalpy (ΔE) are similar for reactions (1) and (3), i.e., 6.4 kJ/mol H₂ and 6.6 kJ/mol H₂ respectively. Similarly, $\Delta H(T = 0 \text{ K})$, which includes zero-point energy, is -19.4 kJ/mol H₂ and -23.4 kJ/mol H₂ for reaction (1) and (3) respectively. The change in free energy, ΔG , is negative in both reactions and also quantitatively similar, with values of -90.1 kJ/mol H₂ and -72.2 kJ/mol H₂ at T = 300 K for reaction (1) and (3) respectively.

We note that in both cases, the negative value of ΔH and ΔG indicates that both Li₄BN₃H₁₀ and CaBNH₆ are thermodynamically unstable compounds, **i.e., their decomposition reactions are exothermic**, at ambient conditions. Although both compounds are stable with respect to decomposition into their constituent amides and borohydrides, these compounds are unstable with respect to decomposition into BN. However, as the Li₄BN₃H₁₀ compound is readily synthesized, it suggests that the kinetics of the BN decomposition pathway are hindered. We speculate that this same kinetic hindrance should allow for the synthesis of our predicted CaBNH₆ phase. A complete list

of the reactions predicted from the GCLP method in the Ca-B-N-H system is given in the Appendix.

The higher temperature reaction (2) observed for $\text{Li}_4\text{BN}_3\text{H}_{10}$ decomposition occurs via Li_3BN_2 formation. Thus one might wonder whether a similar reaction could exist for CaBNH_6 decomposition. Here, while the GCLP study only produces the lowest energy decomposition pathway, which is reaction (3), we have the flexibility to simply remove phases from the calculations whose formation we suspect might be kinetically limited. For example, if the formation of BN is kinetically prohibited, we can remove this phase, and let GCLP predict the lowest decomposition pathway in the absence of BN. These calculations are also detailed in the Appendix, and in the absence of BN, we find that CaBNH_6 can undergo a variety of nearly-degenerate reactions, each of which involves the formation of the recently discovered nitridoborate hydride, $\text{Ca}_2(\text{BN}_2)\text{H}$.⁷¹ Analogous to Li_3BN_2 , there is a ternary Ca-B-N compound with stoichiometry Ca_3BN_3 , but we do not predict CaBNH_6 decomposition into this compound, presumably due to the difference in B:N ratio between CaBNH_6 and Ca_3BN_3 . The Ca_3BN_3 product is more likely from decomposition of a compound with lower B:N ratio in the Ca-(BH_4)-(NH₂) system. As discussed above, the possibility exists for new compounds with lower B:N ratios in this system. An experimental study of this $\text{Ca}(\text{BH}_4)_{2x}(\text{NH}_2)_{2(1-x)}$ system for various B:N ratios would be of considerable interest. Though somewhat speculative, it is possible that the decomposition of CaBNH_6 could occur at lower temperatures than $\text{Li}_4\text{BN}_3\text{H}_{10}$ given the fact that $\text{Ca}(\text{BH}_4)_2$ has ~100 K lower decomposition temperature than LiBH_4 .⁷² Furthermore, since $\text{Ca}(\text{BH}_4)_2$ has been found to be partially reversible, an

experimental test of reversibility in the Ca based amide/borohydride systems would also be of interest.

4. Conclusions

We use a combination of density functional theory (DFT) calculations and a Monte Carlo based crystal structure prediction tool, the Prototype Electrostatic Ground State (PEGS) method, to search for new hydrogen storage compounds in the Ca based mixed amide-borohydride quaternary system. We predict the existence of a new ordered quaternary compound, CaBNH_6 , whose stoichiometry comes from a 1:1 mixture of $\text{Ca}(\text{BH}_4)_2$ and $\text{Ca}(\text{NH}_2)_2$. This Ca-based predicted compound is in a similar material class as the Li-based observed phases Li_2BNH_6 and $\text{Li}_4\text{BN}_3\text{H}_{10}$. Our DFT calculations show that CaBNH_6 is ~ 12.5 kJ/mol Ca (at $T = 0$ K) lower in energy than the mixture of $\text{Ca}(\text{BH}_4)_2$ and $\text{Ca}(\text{NH}_2)_2$. Finite temperature calculations (including vibrational thermodynamics) show that this stability with respect to $\text{Ca}(\text{BH}_4)_2 + \text{Ca}(\text{NH}_2)_2$ persists at finite temperatures as well.

We have also performed a thermodynamic analysis of hydrogen decomposition of our predicted compound using the Grand Canonical Linear Programming (GCLP) method combined with a large database of DFT energies and vibrational thermodynamics. We find that the thermodynamically preferred decomposition reaction for CaBNH_6 involves the formation of BN with a low decomposition enthalpy. Including zero-point effects, we find that the decomposition enthalpy into BN is actually negative, indicating an exothermic decomposition. However, as the analogous reaction is known to be kinetically limited in the Li amide/borohydride case, we suspect that it should be limited in the case of CaBNH_6 as well. Though the decomposition enthalpy is low, the

kinetic behavior of CaBNH_6 decomposition is not yet known. We assert that further experimental investigation of this system is warranted to verify the existence of predicted quaternary compounds in this Ca-B-N-H system. While we have examined the phase stability and thermodynamics of decomposition of CaBNH_6 from DFT, the kinetic barriers that frequently hinder hydrogen release warrant further study to determine a more general understanding of mixed amide-borohydride systems.

Acknowledgement

The authors gratefully acknowledge financial support from the U.S. Department of Energy under Grant No. DE-FC36-08GO18136 and funding from Ford Motor Company under the University Research Program.

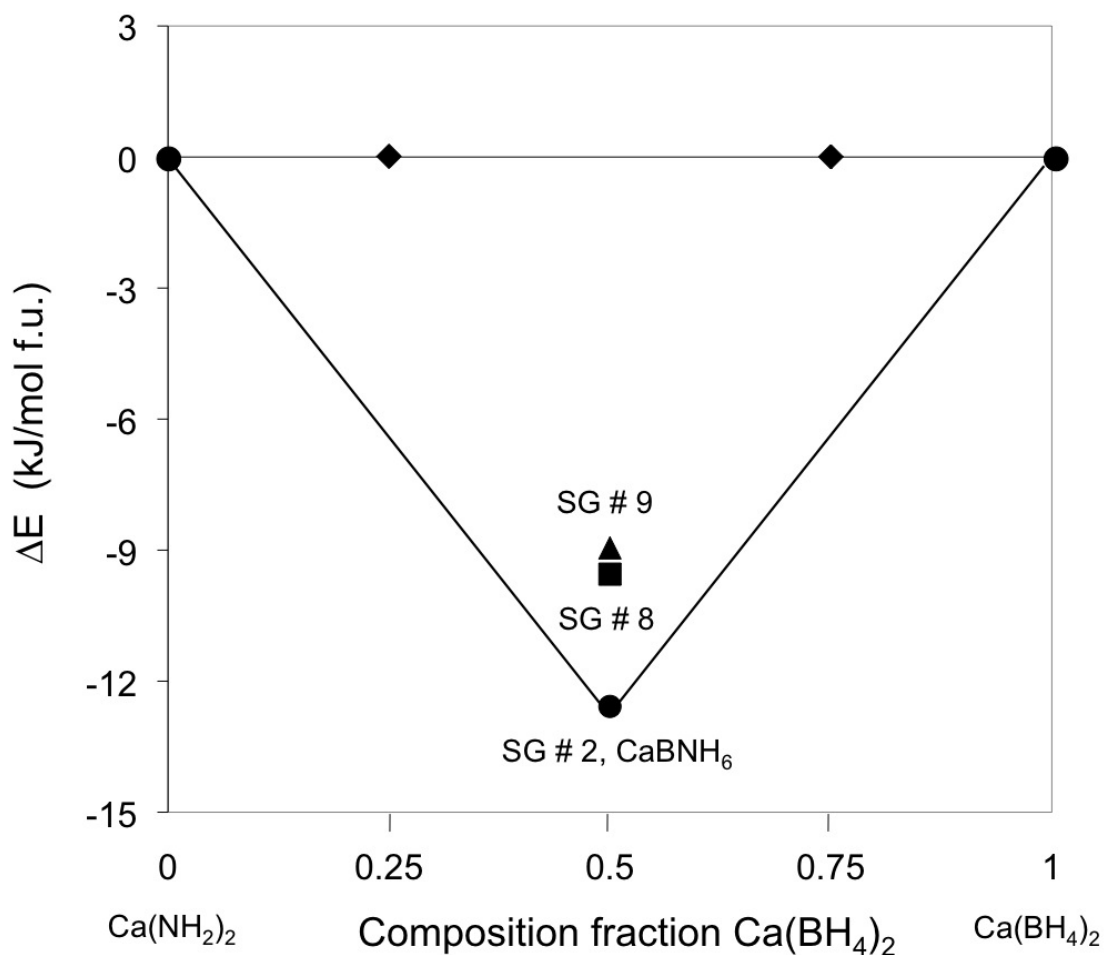


Fig. 1. DFT formation energies of predicted compounds formed between $\text{Ca}(\text{NH}_2)_2$ and $\text{Ca}(\text{BH}_4)_2$ with three compositions, 0.25, 0.5 and 0.75 $\text{Ca}(\text{BH}_4)_2$. For 0.5 composition, three structures with negative formation energies are predicted from PEGS + DFT calculations. The lowest energy structure with SG # 2 is chosen as the crystal structure of 0.50 composition compound, i.e., CaBNH_6 . In contrast, the compounds with compositions 0.25 and 0.75 $\text{Ca}(\text{BH}_4)_2$ (represented in diamonds) are predicted to have positive formation energies. (*For discussion on the positive formation energies, see text*).

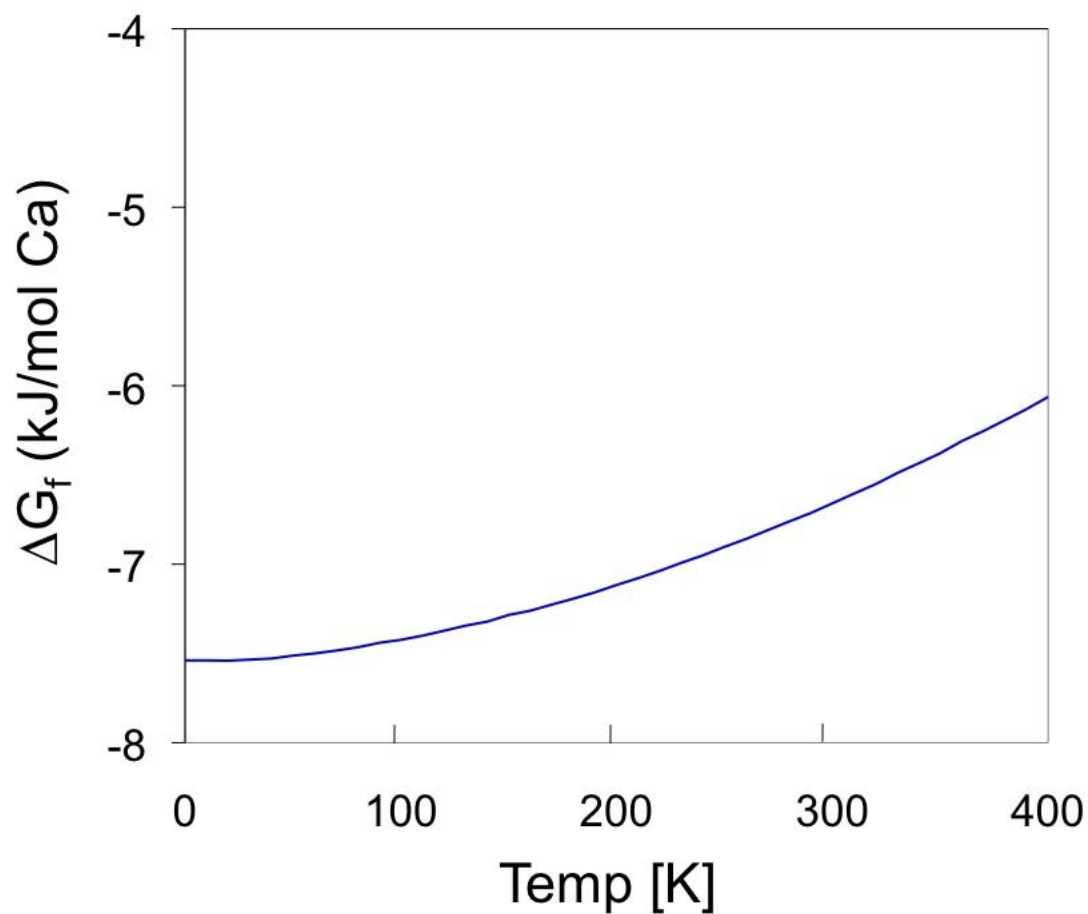


Fig. 2. DFT calculated free energy of formation (ΔG_f) as a function of temperature for CaBNH_6 (see Equation 6 in text) illustrating that the mixed compound is stable against decomposition into its two constituents $\text{Ca}(\text{BH}_4)_2$ and $\text{Ca}(\text{NH}_2)_2$ over a range of temperatures.

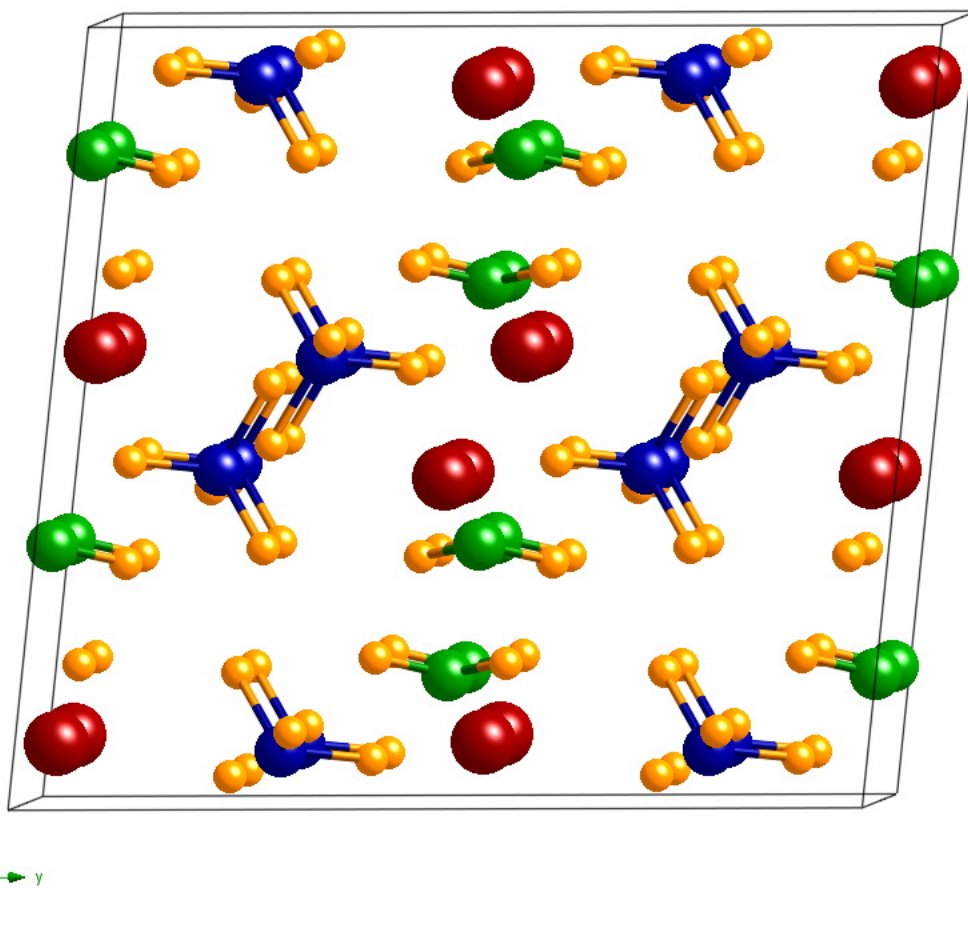


Fig. 3. Crystal structure of the predicted CaBNH_6 phase, obtained from PEGS + DFT calculations. This structure has space group $P\bar{1}$ (# 2) containing two formula units of CaBNH_6 . In the schematic, a $2 \times 2 \times 2$ structure containing 8 unit cells is shown. Ca atoms are shown in red, N in green, B in blue and H in orange.

Table 1

Structural parameters of CaBNH₆ obtained from PEGS + DFT calculations. The space group is $P\bar{1}$ (# 2) with lattice parameters, $a = 5.038 \text{ \AA}$, $b = 5.652 \text{ \AA}$, and $c = 6.956 \text{ \AA}$, and the cell angles, $\alpha = 69.56^\circ$, $\beta = 71.12^\circ$ and $\gamma = 88.93^\circ$.

Ion type	Wyckoff position	x	y	z
Ca	2i	0.169	0.912	0.197
N	2i	0.328	0.034	0.813
B	2i	0.854	0.614	0.723
H1	2i	0.880	0.822	0.579
H2	2i	0.654	0.493	0.726
H3	2i	0.073	0.515	0.684
H4	2i	0.805	0.638	0.899
H5	2i	0.360	0.897	0.744
H6	2i	0.374	0.204	0.685

Table 2

Bond length comparison between the PEGS+DFT obtained CaBNH_6 and the DFT calculated structures of Li_2BNH_6 and $\text{Li}_4\text{BN}_3\text{H}_{10}$

	B-H (Å) in (BH_4) ⁻	N-H (Å) in (NH_2) ⁻	B-cation (Å)	N-cation (Å)
CaBNH_6	1.221- 1.226	1.027, 1.028	2.852 – 3.311	2.533 – 2.541
Li_2BNH_6	1.223- 1.228	1.028	2.422 - 2.518	2.039 – 2.137
$\text{Li}_4\text{BN}_3\text{H}_{10}$	1.223- 1.225	1.027, 1.028	2.375 - 2.592	2.069 – 2.164

Table 3

Comparison of thermodynamically favorable decomposition reactions between CaBNH_6 and $\text{Li}_4\text{BN}_3\text{H}_{10}$.¹⁴ [Static enthalpy at $T = 0 \text{ K}$, ΔE in kJ/mol H_2 , enthalpy including zero point energy, ΔH in kJ/mol H_2 and free energy ΔG in kJ/mol H_2 .] For $\text{Li}_4\text{BN}_3\text{H}_{10}$ decomposition, the values of all four quantities are taken from 14

Reaction	ΔE	$\Delta H (T=0\text{K})$	$\Delta H (T=300\text{K})$	$\Delta G (T=300\text{K})$
$\text{CaBNH}_6 \rightarrow \text{CaH}_2 + \text{BN} + 2\text{H}_2$	6.7	-23.4	-42.1	-72.2
$\text{Li}_4\text{BN}_3\text{H}_{10} \rightarrow 2\text{LiNH}_2 + 2\text{LiH} + \text{BN} + 2\text{H}_2$	6.4	-19.4	-16.1	-90.1

Appendix

The list of the reactions predicted from the GCLP method using the static energies in the Ca-B-N-H system is given below, (ΔE in kJ/mol H₂):

	Reaction	wt. %	ΔE (static energy) (kJ/mol H ₂)
(a)	$\text{Ca}(\text{BH}_4)_2 + (\text{NH}_4)_2\text{B}_{12}\text{H}_{12} \rightarrow 2 \text{BN} + \text{CaB}_{12}\text{H}_{12} + 8\text{H}_2$	6.47	0.5
(b)	$9\text{B}_4\text{H}_{10} \rightarrow 2\text{B}_{18}\text{H}_{22} + 23\text{H}_2$	9.60	0.8
(c)	$\text{CaBNH}_6 \rightarrow \text{CaH}_2 + \text{BN} + 2\text{H}_2$	5.64	6.7
(d)	$10 \text{B}_{18}\text{H}_{22} \rightarrow 9 \text{B}_{20}\text{H}_{16} + 38 \text{H}_2$	3.51	14.4
(e)	$2\text{BN} + 2\text{CaH}_2 + \text{Ca}(\text{NH}_2)_2 \rightarrow \text{Ca}_2\text{BN}_2\text{H} + 4\text{H}_2$	3.22	35.5
(f)	$2(\text{NH}_4)_2\text{B}_{12}\text{H}_{12} \rightarrow 4\text{BN} + \text{B}_{20}\text{H}_{16} + 12 \text{H}_2$	6.75	40.4
(h)	$\text{Ca}(\text{BH}_4)_2 \rightarrow \text{CaB}_2\text{H}_6 + \text{H}_2$	2.87	48.2
(g)	$\text{B}_{20}\text{H}_{16} \rightarrow 20\text{B} + 8\text{H}_2$	6.89	48.8
(i)	$\text{CaH}_2 + \text{Ca}(\text{NH}_2)_2 \rightarrow \text{CaNH} + 2\text{H}_2$	3.50	51.3
(j)	$6\text{CaB}_2\text{H}_6 \rightarrow 5\text{CaH}_2 + \text{CaB}_{12}\text{H}_{12} + 7\text{H}_2$	3.44	60.3
(k)	$\text{CaH}_2 + \text{CaB}_{12}\text{H}_{12} \rightarrow 2\text{CaB}_6 + 7\text{H}_2$	6.25	62.4
(l)	$2\text{NH}_3 \rightarrow \text{N}_2 + 2\text{H}_2$	17.65	65.4
(m)	$\text{Ca}_2\text{BN}_2\text{H} + \text{Ca}(\text{NH}_2)_2 \rightarrow \text{BN} + 3\text{CaNH} + \text{H}_2$	1.04	83.1
(n)	$\text{CaH}_2 + \text{CaNH} \rightarrow \text{Ca}_2\text{NH} + \text{H}_2$	2.06	86.3
(o)	$\text{CaB}_{12}\text{H}_{12} \rightarrow 6\text{B} + \text{CaB}_6 + 6\text{H}_2$	6.60	91.6

The volumetric density from the decomposition of CaBNH₆ via reaction (c) is found to be 76.68 g H₂/ L.

The GCLP method allows us to find low-energy decomposition reactions for a given set of possible phases, some of which may occur only under specific conditions. For instance, the formation of BN is kinetically limited such that Reaction (1) (in the text) is predicted to occur at low temperature, but is not observed experimentally. We look for analogous reactions in the case of CaBNH₆ decomposition under circumstances where BN is not allowed to form. In the following, reactions (aa) – (dd) are the CaBNH₆

decomposition reactions that are predicted by the GCLP in the absence of BN as a byproduct. The volumetric densities obtained in the order of these reactions are 96.20, 91.30, 69.58 and 69.01 g H₂/L. The reactions (ee) – (tt) are the other hydrogen-release reactions observed in the absence of BN, among which (ee) – (mm) are the reactions that are also observed above.

	Reaction	wt. %	ΔE (static energy) (kJ/mol H ₂)
(aa)	$2\text{CaBNH}_6 + \text{Ca}(\text{NH}_2)_2 + \text{CaH}_2 \rightarrow 2\text{Ca}_2\text{BN}_2\text{H} + 8\text{H}_2$	6.25	21.1
(bb)	$9\text{CaBNH}_6 + 3\text{Ca}(\text{NH}_2)_2 \rightarrow 6\text{Ca}_2\text{BN}_2\text{H} + \text{B}_3\text{N}_3\text{H}_6 + 27\text{H}_2$	6.32	22.6
(cc)	$4\text{CaBNH}_6 + \text{CaH}_2 \rightarrow 2\text{Ca}_2\text{BN}_2\text{H} + \text{Ca}(\text{BH}_4)_2 + 8\text{H}_2$	4.91	25.8
(dd)	$15\text{CaBNH}_6 \rightarrow 6\text{Ca}_2\text{BN}_2\text{H} + 3\text{Ca}(\text{BH}_4)_2 + \text{B}_3\text{N}_3\text{H}_6 + 27\text{H}_2$	5.08	26.8
(ee)	$9\text{B}_4\text{H}_{10} \rightarrow 2\text{B}_{18}\text{H}_{22} + 23\text{H}_2$	9.60	0.8
(ff)	$10\text{B}_{18}\text{H}_{22} \rightarrow 9\text{B}_{20}\text{H}_{16} + 38\text{H}_2$	3.51	14.4
(gg)	$\text{B}_{20}\text{H}_{16} \rightarrow 20\text{B} + 8\text{H}_2$	6.89	48.8
(hh)	$\text{Ca}(\text{BH}_4)_2 \rightarrow \text{CaB}_2\text{H}_6 + \text{H}_2$	2.87	48.2
(ii)	$\text{CaH}_2 + \text{Ca}(\text{NH}_2)_2 \rightarrow \text{CaNH} + 2\text{H}_2$	3.50	51.3
(jj)	$6\text{CaB}_2\text{H}_6 \rightarrow 5\text{CaH}_2 + \text{CaB}_{12}\text{H}_{12} + 7\text{H}_2$	3.44	60.3
(kk)	$\text{CaH}_2 + \text{CaB}_{12}\text{H}_{12} \rightarrow 2\text{CaB}_6 + 7\text{H}_2$	6.25	62.4
(ll)	$2\text{NH}_3 \rightarrow \text{N}_2 + 2\text{H}_2$	17.65	65.4
(mm)	$\text{CaH}_2 + \text{CaNH} \rightarrow \text{Ca}_2\text{NH} + \text{H}_2$	2.06	86.3
(nn)	$3\text{Ca}(\text{BH}_4)_2 + 3(\text{NH}_4)_2\text{B}_{12}\text{H}_{12} \rightarrow 3\text{CaB}_{12}\text{H}_{12} + 2\text{B}_3\text{N}_3\text{H}_{12} + 12\text{H}_2$	3.23	3.4
(oo)	$\text{B}_3\text{N}_3\text{H}_{12} \rightarrow \text{B}_3\text{N}_3\text{H}_6 + 3\text{H}_2$	6.94	16.2
(pp)	$15\text{Ca}(\text{BH}_4)_2 + 4\text{B}_3\text{N}_3\text{H}_6 \rightarrow 6\text{Ca}_2\text{BN}_2\text{H} + 3\text{CaB}_{12}\text{H}_{12} + 51\text{H}_2$	7.46	45.9
(qq)	$3(\text{NH}_4)_2\text{B}_{12}\text{H}_{12} \rightarrow 30\text{B} + 2\text{B}_3\text{N}_3\text{H}_6 + 24\text{H}_2$	9.00	60.0
(rr)	$6\text{Ca}_2\text{BN}_2\text{H} + 13\text{CaB}_{12}\text{H}_{12} \rightarrow 25\text{CaB}_6 + 4\text{B}_3\text{N}_3\text{H}_6 + 69\text{H}_2$	4.47	71.0
(ss)	$12\text{Ca}(\text{NH}_2)_2 + 2\text{B}_3\text{N}_3\text{H}_6 \rightarrow 9\text{N}_2 + 6\text{Ca}_2\text{BN}_2\text{H} + 27\text{H}_2$	5.26	86.9

-
- ¹ Yang J., Sudik A., Wolverton C. and Siegel D. J., *Chem. Soc. Rev.* **39**, 656-675, 2010.
- ² G. Sandrock, *J. Alloys Compd.* **877**, 293–295, 1999.
- ³ B. Sakintuna, F. Lamari-Darkrim and M. Hirscher, *Int. J. Hydrogen Energy* **32**, 1121, 2007.
- ⁴ A. Zuttel, S. Rentsch, P. Fisher, P. Wenger, P. Sudan, Ph. Mauron and Ch. Emmenegger *J. Alloys Compd.*, **356**, 515, 2003.
- ⁵ A. Zuttel, P. Wenger, S. Rentsch and P. Sudan, *J. Power Sources* **118**, 1, 2003.
- ⁶ Y. Nakamori, H. Li, K. Miwa, S. Towata and S. Orimo, *Mater. Trans.* **47**, 1898, 2006.
- ⁷ B. Bogdanovic' and M. Schwickardi, *J. Alloys Compd.* **253–254**, 1 1997.
- ⁸ P. Chen, Z. T. Xiong, J. Z. Luo, J. Y. Lin and K. L. Tan, *Nature* **420**, 302, 2002.
- ⁹ H. Li, M. Eddaoudi, M. O'Keeffe and O. M. Yaghi, *Nature* **402**, 276, 1999.
- ¹⁰ F. H. Stephens, V. Pons and R. T. Baker, *Dalton Trans.* 2613, 2007.
- ¹¹ Pinkerton F. E., Meisner G. P., Meyer M. S., Balogh M. P. and Kundrat M. D., *The J. Phys. Chem. B Lett.* **109**, 6-8, 2005.
- ¹² Meisner G. P., Scullin M. L., Balogh M. P., Pinkerton F. E. and Meyer M. S., *J. Phys. Chem. B* **110**, 4186-4192, 2006.
- ¹³ Wu H., Zhou W., Udovic T. J., Ruch J. J. and Yildirim T., *Chem. Mater.* **20**, 1245-1247 (2008).
- ¹⁴ Siegel D. J., Wolverton C., and Ozolins V., *Phys. Rev. B* **75**, 014101, (2007).
- ¹⁵ Aoki M., Miwa T., Noritake T., Kitahara Y., Nakamori S., Orimo S., and Towata S., *Applied Physics A: Mater. Sci. Process.* **80**,1409 (2005).
- ¹⁶ Nakamori Y., Ninomiya A., Kitahara G., Aoki M., Noritake T., Miwa K., Kojima Y., and Orimo S., *J. Pow. Sour.*, **155**, 447, 2006.
- ¹⁷ Singer J. P., Meyer M. S., Speer R. M., Fisher J. E. and Pinkerton F. E., *J. Phys. Chem. C* **113**, 18927-18934, 2009.
- ¹⁸ Farrell D. E., Shin D. and Wolverton C., *Phys. Rev. B* **80**, 224201, 2009.
- ¹⁹ Hoang K. and Van de Walle C. G., *Phys. Rev. B* **80**, 214109, 2009.
- ²⁰ Pinkerton F. E. and Meyer M. S., *J. Phys. Chem. C* **113**, 11172-11176, 2009.
- ²¹ Majzoub E. H. and Ozolins V., *Phys. Rev. B* **77**, 104115 (2008).
- ²² Akbarzadeh A. R., Ozolins V. and Wolverton C., *Adv. Mater.* **19**, 3233 (2007).
- ²³ S. V. Alapati, J. K. Johnson and D. S. Sholl, *J. Phys. Chem. B* **110**, 8789, 2006.
- ²⁴ Ozolins V, Akbarzadeh AR, Gunaydin H, Michel K, Wolverton C and Majzoub E. H., *First-Principles Computational Discovery of Materials for Hydrogen Storage J. Phys.: Conf. Ser.* **180**, 012076, 2009,
- ²⁵ Peles A and Van de Walle G., *Phys. Rev. B* **76**, 214101 (2007).
- ²⁶ Marashdeh A., Olsen R. A., Lovvik O. M. and Kroes G-J., *Chem. Phys. Lett.* **426**, 180, (2006).
- ²⁷ Miwa K., Aoki M., Noritake T., Ohba N., Nakamori Y., Towata S-I, Zuttel A. and Orimo S-I., *Phys. Rev. B* **74**, 155122 (2006).
- ²⁸ Ramzan M. and Ahuja R., *J. Appl. Phys.* Ramzan **106**, 016104, (2009).
- ²⁹ Hector L.G., Herbst J. F. and Kresse G. *Phys. Rev. B* **76**, 014121 (2007).
- ³⁰ de Dompablo M., Ceder G., *J Alloys and Comp.* **364**, 6, (2004).

-
- ³¹ Wolverton C., Ozolins V. and Asta M, Phys. Rev. B **69**, 144109, (2004).
- ³² Wolverton C. and Ozolins V., Phys. Rev. B **75**, 064101 (2007).
- ³³ Siegel D., Wolverton C. and Ozolins V., Phys. Rev. B **76**, 134102 (2007)
- ³⁴ Ozolins V., Majzoub E. H and Wolverton C., J. Am. Chem Soc. **131**, 230 (2009).
- ³⁵ Zhang Y., Majzoub E. H, Ozolins V. and Wolverton C. Phys. Rev. B **82**, 174107 (2010).
- ³⁶ Wolverton C., Siegel D.J., Akbarzadeh A.R. and Ozolins V., J. Phys-Cond. Matt. **20**, 064228 (2008).
- ³⁷ Weidenthaler C., Pommerin A., Felderhoff M., Sun W., Wolverton C., Bogdanovic B. and Schueth F., J. Am. Chem. Soc. **131**, 16735 (2009).
- ³⁸ F. Buchter, Z. Łodziana, A. Remhof, O. Friedrichs, A. Borgschulte, Ph. Mauron, A. Zuttel, D. Sheptyakov, G. Barkhordarian, R. Bormann, K. Chłopek, M. Fichtner, M. Sørby, M. Riktor, B. Hauback and S. Orimo J. Phys. Chem. B **112**, 8042 (2008).
- ³⁹ K. Miwa, N. Ohba, and S.-I. Towata, Y. Nakamori and S.-I. Orimo Phys. Rev. B **69**, 245120 (2004).
- ⁴⁰ K. Miwa, N. Ohba, and S.-I. Towata, Y. Nakamori and S.-I. Orimo and Phys. Rev. B **71**, 195109 (2005).
- ⁴¹ J. F. Herbst and L. G. Hector Jr, Phys. Rev. B **72**, 125120 (2005).
- ⁴² L. G. Hector Jr and J. F. Herbst, J. Phys.: Condens. Matter **20**, 064229 (2008).
- ⁴³ L. G. Hector Jr, J. F. Herbst and T. W. Capehart, J. Alloys. And Comp. **353**, 74 (2003).
- ⁴⁴ O. M. Løvvik and S. M. Opalka, Phys. Rev. B **71**, 054103 (2005).
- ⁴⁵ A. Marashdeh, R. A. Olsen, O. M. Løvvik and G.-J. Kroes, Chem Phys. Lett. **426**, 180 (2006).
- ⁴⁶ O.M. Løvvik, O Swang and S. M. Opalka, J. Mater. Res., **20**, 3199 (2005).
- ⁴⁷ O.M. Løvvik and S. M. Opalka, Phys. Rev. B **72**, 073201 (2005).
- ⁴⁸ J. S. Hummelshøj, et al, J. Chem. Phys. **131**, 014101 (2009).
- ⁴⁹ S. V. Alapati, J. K. Johnson, and D. S. Sholl, J. Phys. Chem. C **112**, 5258 (2008).
- ⁵⁰ S. V. Alapati, J. K. Johnson, and D. S. Sholl, Phys. Chem. Chem. Phys. **9**, 1438 (2007).
- ⁵¹ B. Dai, D. S. Sholl, J. K. Johnson, J. Phys. Chem C **112**, 4391 (2008).
- ⁵² Diyabalanage H. V. K., Shrestha R. P., Semelsberger T. A., Scott B. L., Bowden M. E., Davis B. L., Burrell A. K., Angew. Chem.-Inter. Edi. **46**, 8995 (2007).
- ⁵³ Wu H., Zhou W. and Yildirim T., J. Am. Chem. Soc. **130**, 14834 (2008).
- ⁵⁴ Ozolins V., Majzoub E. H. and Wolverton C., Phys. Rev. Lett. **100**, 135501 (2008).
- ⁵⁵ Zhang Y., Ozolins V. and Wolverton C., (in preparation).
- ⁵⁶ Seballos L., Zhang J. Z., Ronnebro E., Herberg J. L. and Majzoub E. H., J. Alloys and Comp. **476**, 446 (2009).
- ⁵⁷ Kim C., Hwang S.-J., Bowman R. C., Reiter J. W., San J. A., Kulleck J. G., Kabbour H., Majzoub E. H. and Ozolins V., J. Phys. Chem. C **113**, 9956 (2009).
- ⁵⁸ Aidhy D.S. and Wolverton C., Phys. Rev. B **83**,144111 (2011).
- ⁵⁹ Bader R., Atoms and Molecules: A Quantum Theory, Oxford University Press, NY, 1990.
- ⁶⁰ Kittel C., Introduction to Solid State Physics, Seventh Edition, Wiley.
- ⁶¹ Kreese G. and Hafner J., Phys. Rev. B **47**, 558 (1993).
- ⁶² Kreese G. and Joubert D., Phys. Rev. B **59**, 1758 (1999).
- ⁶³ Perdew J. P. and Wang Y., Phys. Rev. B **45**, 13244 (1992).

-
- ⁶⁴ Blochl P. E., Phys. Rev. B **50**, 17953 (1994).
- ⁶⁵ Monkhorst-H. J. and Pack J. D., Phys. Rev. B **13**, 5188 (1976).
- ⁶⁶ Wallace D. C., Thermodynamics of Crystals (John Wiley and Sons, NY, 1972).
- ⁶⁷ Rickman J. M. and LeSar R., Annu. Rev. Mater. Res. **32**, 195 (2002).
- ⁶⁸ Soulie J-Ph., Renaudin G., Cerny R. and Yvon K., J. Alloys and Comp. **346**, 200-205, 2002.
- ⁶⁹ Filinchuk Y. E., Yvon K., Meisner G. P., Pinkerton F. E., and Balogh M. P., Inorg. Chem. **45**, 1433 (2006).
- ⁷⁰ Chater P. A., David W. I. F., Johnson S. R., Edwards P. P., and Anderson P. A., Chem. Commun. **23**, 2439 (2006).
- ⁷¹ Somer M., Yaren O., Reckeweg O., Prots Yu. M. and Carillo-Cabrera W., Z. Anor. Allg. Chem. **630**, 1068-1073 (2004).
- ⁷² Filinchuk Y., Ronnebro E. and Chandra D., Acta Mater. **57**, 732-738, 2009.